# Numerical Modelling and Performance Assessment of MicroFluidic Glazing (MFG)

# Yangkong ZHOU Polytech'Lab, UPR UCA 7498

Université Cote d'Azur Sophia Antipolis, France; Technology Energy Building Environment research group, Energy Department Politecnico di Torino, Torino, Italy e-mail: yangkong.zhou@univ-cotedazur.fr, yangkong.zhou@polito.it

# Manuela BARACANI

Technology Energy Building Environment research group, Energy Department Politecnico di Torino, Torino, Italy e-mail: manuela.baracani@polito.it

# Fabio FAVOINO

Technology Energy Building Environment research group, Energy Department Politecnico di Torino, Torino, Italy e-mail: fabio.favoino@polito.it

#### Stefano FANTUCCI

Technology Energy Building Environment research group, Energy Department Politecnico di Torino, Torino, Italy e-mail: stefano.fantucci@polito.it

# Mohamad IBRAHIM Polytech'Lab, UPR UCA 7498

Université Cote d'Azur Sophia Antipolis, France; e-mail: mohamad.ibrahim@univ-cotedazur.fr

# Erwin FRANQUET Polytech'Lab, UPR UCA 7498

Université Cote d'Azur Sophia Antipolis, France; e-mail: erwin.franquet@univ-cotedazur.fr

# Valentina SERRA\*

Technology Energy Building Environment research group, Energy Department Politecnico di Torino, Torino, Italy e-mail: stefano.fantucci@polito.it

#### **ABSTRACT**

Advanced Fenestration Systems (AFS) have been developed to fully exploit both the thermal and optical components of solar radiation. One such AFS, MicroFluidic Glazing (MFG), features fluid flow within laminated micro-channels, enabling the harvesting of solar radiation, transmission of visible light, and adjustment of indoor thermal environments. Although numerous experimental studies have assessed the performance of MFG, developing a numerical thermal model for

\_

<sup>\*</sup> Corresponding author

complicated simulations under various working conditions and particularly building-level evaluations remains challenging. In this study, a Thermal Capacitance-Resistance (RC) numerical model for a triple-glazing type MFG is developed and validated by the experimental data obtained at a flow rate of 9.6 l/h (0.00062m/s) with a component size of 0.68m\*0.58m. Furthermore, the performance of this model is evaluated under different control strategies at the building level, utilizing a generic co-simulation framework previously proposed. The annual solar radiation harvesting ratio under different constant and dynamic control show a relatively low idea heating and cooling need, with constant control strategy ratios of 23.08% and dynamic control strategy ratios of 24.26%. These figures demonstrate the substantial potential advantages in energy saving and harvesting of MFG.

# **KEYWORDS**

Microfluidic Glazing, Advanced Fenestration Systems, Numerical model, co-simulation

#### INTRODUCTION

The building industry is responsible for approximately 40% of total energy consumption and 36% of energy-related greenhouse gas emissions in the European Union (EU) [1]. In response to these environmental challenges, the EU has set the objective of moving to Nearly Zero-Energy Buildings (NZEBs) starting from 2020 [2]. The building envelope plays a crucial role in building performance, with the fenestration system normally representing the most vulnerable point. Consequently, researchers are exploring Advanced Fenestration Systems (AFS) that capitalize on both thermal and optical components of solar radiation to achieve energy efficiency, reduced CO<sub>2</sub> emissions, and enhanced indoor space comfort simultaneously.

Water-filled Glass (WFG) is a promising AFS technology, comprising a transparent double or triple glazing system that utilizes water infill to harvest solar radiation, thereby enhancing thermal performance [3]. Initial studies on static water storage envelopes demonstrated the thermal benefits of WFG for ultra-low energy buildings [4], [5]. However, the static nature of the water limits its performance when long extreme weather condition occurs, limiting real-world implementation and application [6]. To optimize WFG performance, researchers developed a new configuration that allows the infilled water to circulate. However, challenges related to sealing, water pressure, and pumping energy consumption remain to be addressed [3]. In order to fully harness the potential of WFG technology, an advanced and modularized WFG system, Microfluid Glazing (MFG), was developed. MFG features an array of micro-capillaries that enable fluid flow through channels to harvest heat, while a thin cover sheet minimizes overall weight and thickness, subsequently reducing pumping energy demand [7]. Previous experimental research of this technology involves the normal glass sheet with a triple glazing unit containing the capillary layer, has demonstrated the adjustment of the flowrate the great potential of reducing the glazing temperature and optimizing the performance through the change of the flowrate [8]. Despite the potential benefits of Microfluid Glazing (MFG) technology, its complexities and intricacies have posed challenges for integration into existing state-of-the-art Building Performance Simulation (BPS) tools. There are already some researches about the numerical model about the MFG technology. Simplified numerical models were built to evaluate its performance based on window area at building level with micro-fluidic layer at exterior or interior layer [9] [10], but the structure that put the microfluidic layer in the middle of the triple glazing unit hasn't been researched. There is even a more complicated model to evaluate the non-uniform temperature distribution across the micro-fluidic

layer [11], but for evaluating at a building level, it's too complicated and will cost too much simulation time. Consequently, the lack of numerical models for this type of MFG in these BPS tools hampers the evaluation and optimization of the system with respect to various parameters and diverse climatic conditions at the whole-building level.

To fully understand the performance and potentials of MFG applied to real buildings, simulations with BPS tools are needed. The objective of this work is to develop and validate a numerical model for a triple glazing MFG and assess its performance at the whole-building level. In this paper, a thermal network for MFG based on the triple glazing unit at the beginning. Subsequently, experimental data obtained from previous research is utilized to validate the numerical model. Finally, an evaluation of this technology is conducted using the BESTTEST building model within a generic co-simulation infrastructure, allowing for a comprehensive assessment of MFG's potential impact on building thermal performance.

# **METHODOLOGY**

Given the absence of specific models for certain components within state-of-the-art BPS tools, it is essential to develop numerical models that can be used and integrated with these tools. In the case of the MFG technology studied in this research, which is a transparent configuration (the exact configuration is shown in Figure 1, the focus of this paper is solely on its thermal and energy performance for the whole building. Consequently, we developed a thermal Capacitance-Resistance (RC) numerical model based on a simplified thermal network The numerical model is validated using experimental data of a mock-up unit conducted at the Department of Energy (DENERG) at Politecnico di Torino [8] for one working condition. Finally, the MFG performance is assessed at Building scale under different operating conditions considering the test case BESTTEST via a generic co-simulation method that can be employed for various AFS numerical models.

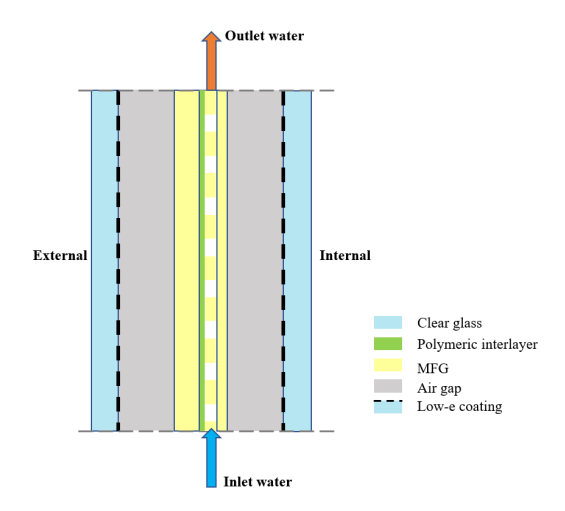


Figure 1. Triple glazing MFG configuration

# Thermal network and numerical model

The MFG combines the triple glazing system and the MFG layer. As depicted in Figure 2, the thermal network is constructed in the horizontal direction by dividing each of the three glazing layers into three nodes (the two surfaces and the central point of the glazing).

The thermal resistances of the system encompass the thermal resistance due to conductive heat transfer (R<sub>cd.i</sub>) within the j glass layer, the thermal resistance due to the convective heat transfer (R<sub>cv,k</sub>) in the k air cavity layer and both external and internal layers, as well as the thermal resistance due to radiative heat transfer(R<sub>rd,k</sub>) within the k air cavity. The equations are shown from equation (1)~(3).  $S_i$  (m) is the glass thickness of the j layer;  $\lambda_i$  (W/m. K) is the thermal conductivity of j glass layer.  $h_{c,k}(W/m^2)$  and  $h_{r,k}(W/m^2)$  are the convective and radiative heat transfer coefficient in the k air cavity.

$$R_{cd,j} = \frac{S_j}{2\lambda_j} \tag{1}$$

$$R_{cv,k} = \frac{1}{h_{ck}} \tag{2}$$

$$R_{cd,j} = \frac{s_j}{2\lambda_j}$$

$$R_{cv,k} = \frac{1}{h_{c,k}}$$

$$R_{rd,k} = \frac{1}{h_{r,k}}$$

$$(3)$$

In the thermal model, The external and internal heat transfer coefficient are  $h_e(W/m^2)$  and  $h_i(W/m^2)$ ;  $T_{ae}(^{\circ}C)$ ,  $T_{ai}(^{\circ}C)$ , represent outdoor temperature and inside temperature, respectively. The thermal capacity of each glass layer, Cgj (J/kg. K), and the heat gained from solar radiation, which equals the intensity of the incident solar radiation,  $I_{inc}(W/m^2)$ , multiplied by the absorptance of each glass layer  $(\alpha_i)$ , are also considered. The  $\alpha_i$  is calculated from WINDOW software, which has already considered the reflection and absorption of incident solar radiation at each layer. For the MFG layer, the thermal behavior of the flowing fluid within the channel is fully accounted for by including the fluid heat transfer coefficient h<sub>w</sub>(W/m<sup>2</sup>), which is the reciprocal of the  $R_w$  (m<sup>2</sup>.K/W), and the thermal capacity of the fluid in the MFG layer,  $C_w$ (J/kg. K).

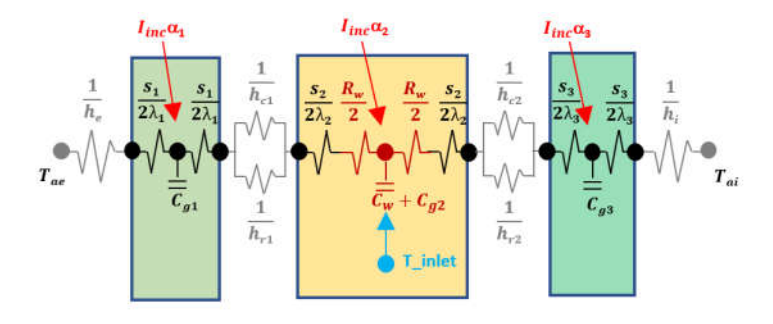


Figure 2. MFG thermal network scheme

The convective heat transfer coefficient h<sub>c,k</sub> within k gas filled layer is calculated through the equation (4) according to the methodology proposed by ISO15099 standard [12]. Here, Nu<sub>k</sub>

represents the dimensionless Nusselt number of the k cavity,. The thermal conductivity of the gas fill is denoted by  $\lambda_k(W/m. K)$ , and the thickness of k cavity is represented by  $S_k(m)$ .

$$h_{c,k} = Nu_k \left(\frac{\lambda_k}{S_k}\right) \tag{4}$$

The radiative heat transfer coefficient,  $h_{r,k}$  within k gas filled layer is calculated through the equation (5) according to the Stefan-Boltzmann law. In this equation, the  $\sigma(W/(m^2K^4))$  is Stefan-Boltzmann constant,  $\epsilon_{k,l}$  and  $\epsilon_{k,r}$  denote the emissivity of the left and right surfaces of the k cavity, and  $T_l$ ,  $T_r$  represent the temperatures of the left and right surfaces of the k cavity, respectively.

$$h_{r,k} = \sigma \left(\frac{1}{\varepsilon_l} + \frac{1}{\varepsilon_r} - 1\right)^{-1} * (T_l^2 + T_r^2)(T_l + T_r)$$
(5)

The fluid heat transfer coefficient  $h_w$  within the MFG layer is calculated through the equation (6). In this equation, the  $Nu_{fc}$  is the dimensionless Nusselt number of the fluid channel, which is calculated according to the shape of the micro-channel [13].  $\lambda_f$  denote the thermal conductivity of the flowing fluid, Dh (m) is the hydraulic diameter of flowing fluid,. Considering the range of flow velocities considered, the length of hydrodynamic entrance and thermal entrance are much shorter than the length of the channels constituting the microfluidic glass,  $h_w$  was considered constant throughout the length of the channel.  $\rho_w(kg/m^3)$ ,  $c_w(J/kg.K)$  represent the density and capacity of fluid, respectively.  $v_w(m/s)$  is the velocity of the fluid inside the micro-fluid channel.

$$h_w = Nu_{fc} \left( \frac{\lambda_f}{Dh} \right) \tag{6}$$

The relating parameters about the properties of different layers comes from both experiment under 9.3 l/h with component size of 0.68m\*0.58m [8] or WINDOW software [14]. Some important parameters about MFG layer used in the MFG system are shown in Table 1. To make sure the thermal network could be calculated feasibly, we simplified the micro channels to a water layer that has the same cross-sectional area inside the MFG layer  $S_f$ .

Table 1. Parameters at MFG layer

T <sub>inlet</sub> (K)	$\rho_w = (\text{kg.m}^3)$	$C_w$ $(J/kg.K)$	$\lambda_f$ (W/m.K)	$D_h$ $(m)$	$S_f$ $(m)$	$Nu_{fc}$	$V_w (m/s)$	$h_w = (W/m^2)$
293	1063	3496.1	0.41	0.00188	0.00063	3.96	0.00062	863.07

The logic of numerical model is based on the thermal network and the work flow in shown in Figure 3. In the horizontal direction, the thermal network is constructed by dividing each of the three glazing layers into three nodes (the two surfaces and the central point of the glazing), with each node's heat balance being considered. For the vertical direction, the network is divided into 10 nodes, and the temperature increase in the micro-fluid layer is accounted for by using the middle point temperature of the micro-fluid layer at the previous position as the initial temperature for the subsequent position, followed by a horizontal iteration, which is shown in equation (7). The heat

balance equation from horizontal calculating node at the first glazing layer is shown in the equation from (8)~(10), the other nodes are similar to the one in the first glazing layer.  $T_i^t$  (°C),  $T_i^{t-1}$  (°C) represent the temperature of horizontal i node at t and t – 1 time step, respectively;  $\Delta t(s)$  is calculating time step;  $T_5^{t,i-1}$  (°C),  $T_5^{t,i}$  (°C) represent the micro-fluid temperature at vertical position Y-1 and Y, respectively;  $\Delta y(m)$  is the vertical distance between two vertical calculating nodes. The dynamic boundary condition is under real weather data but it has the  $T_{inlet}$ =20°C and  $T_{inlet}$ =11 W/m², but  $T_{inlet}$ =20°C and  $T_{inlet}$ =11 W/m² to 0.32 to fully express the aging and experimental error problem.

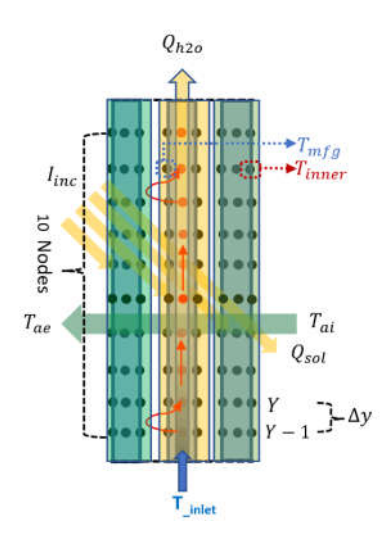


Figure 3. Numerical simulating model

$$(T_4^t - T_5^t) \left(\frac{1}{S_2/(2*\lambda_2)}\right) + (T_6^t - T_5^t) \left(\frac{1}{S_2/(2*\lambda_2)}\right) + (T_5^{t-1} - T_5^t) \left(\frac{\rho_{glass,2} c_{glass,2} S_2}{\Delta t}\right) + I_{inc} * \alpha_2 + \left(T_5^{t,Y-1} - T_5^{t,Y}\right) \left(\frac{\rho_{w} c_w v_w s_w}{\Delta v}\right) = 0$$
 (7)

$$(T_{ae} - T_1^t) \left(\frac{1}{1/h_e}\right) + (T_2^t - T_1^t) \left(\frac{1}{S_1/(2*\lambda_1)}\right) = 0$$
(8)

$$(T_1^t - T_2^t) \left( \frac{1}{\frac{S_1}{2*\lambda_1}} \right) + (T_3^t - T_2^t) \left( \frac{1}{\frac{S_1}{2*\lambda_1}} \right) + (T_3^{t-1} - T_2^t) \left( \frac{\rho_{glass,1} c_{glass,1} s_1}{\Delta t} \right) + I_{inc} * \alpha_1 = 0$$
 (9)

# Validation indicators

In this study, the validation between the dynamic numerical model and the experimental data is conducted, considering the condition under a water flow rate of 9.3 l/h (velocity of 0.00062 m/s). Three key indicators were selected as validation metrics in this research: 1) T<sub>inner</sub>(the temperature

of the inner surface layer, taken the value from top position); 2)  $T_{mfg}$  (Temperature at the top position of MFG layer); and 3)  $T_{difference}$  ( $T_{outlet} - T_{inlet}$ ). To quantify the error between the simulation results and experimental data for these indicators, linear regression, Mean Absolute Error (MAE), Root Mean Square Error (RMSE), Standard Deviation (SD), and Maximum Absolute Error (MaxAE) were employed.

# **Building level evaluation**

Evaluating the real-world performance of MFG and other Advanced Façade Systems (AFS) necessitates conducting simulations within a realistic building model. However, due to the complexities of AFS, there are no readily available models within Building Performance Simulation (BPS) tools [15]. Consequently, co-simulation is required to establish a connection between AFS models and BPS tools [16].

In the previous research, a Python-based co-simulation method was developed for AFS, allowing for interactions at both thermal and optical levels [17]. For this study, the workflow is depicted in Figure 4, and only the thermal aspect is considered, with solar radiation transmittance held constant at a value of  $\tau$ =0.4, based on experimental data. A simplified thermal zone model, according to the BEST TEST Case600, was selected as a representative test building under the climate condition of Torino [18], as illustrated in Figure 4. To fully express the performance of the MFG in the whole building scale, the south wall features a transparent component, with MFG dimensions adapting from 0.68m (width) x 0.58m (height) to 7.8m (width) x 2.5m (height). Notably, despite these alterations in size, the inherent properties of each layer remain consistent throughout. Heating setpoints are 20°C (working hours) and 18°C (non-working hours), while cooling setpoints are 26°C (working hours) and 30°C (non-working hours). No heating is provided during the summer, and the infiltration rate varies from 0.5 AC/h to 10 AC/h to simulate summer-free cooling (night ventilation). Parameters were updated based on simulation results from the WINDOW software, assuming a clear Microfluidic Glazing unit. Three conditions were selected for comparison: 1) Constant control strategy (0.00062 m/s); 2) Dynamic control strategy, as shown in Table 2. The calculation time step is 10 minutes, and  $T_{inlet} = 15$ °C.

The MFG performance at the building level will be analyzed from three perspectives: 1)  $T_{inner}$  (the inner surface temperature of the MFG) and  $T_{ai}$  in typical summer and winter season; 2) Ideal heating/cooling energy need per area, and annual solar radiation harvesting ratio ( $\frac{Q_{har}}{A_{win}*I_{inc}}$ ,  $Q_{har}$ ,  $A_{win}$  means annul total harvested solar radiation and area of the MFG).

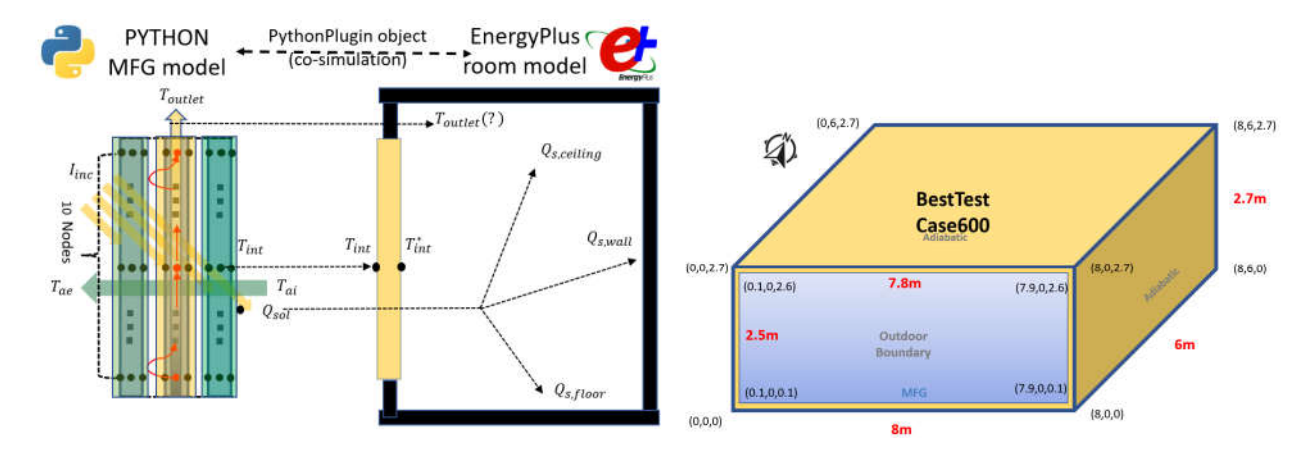


Figure 4. Co-simulation logic and test building model.

Table 2. Dynamic control strategy in different season

Summer (6-8)	Winter (11-2)
If $I_{inc}$ <50W/m <sup>2</sup> , 1.3*10 <sup>-4</sup> m/s	If $I_{inc}$ <50 W/m <sup>2</sup> , 1.3*10 <sup>-4</sup> m/s
If 50 W/m <sup>2</sup> $< I_{inc}$ , 1.6*10 <sup>-3</sup> m/s	If $50 \text{ W/m}^2 < I_{inc} < 250 \text{ W/m}^2$ , $6.2*10^{-4} \text{m/s}$
	If $250 \text{ W/m}^2 < I_{inc}$ , $1.07*10^{-3} \text{ m/s}$

# NUMERICAL MODEL VALIDATION

The dynamic model simulation results, presented in Figure 5, are compared with the experimental data for enhanced clarity. The data displayed are the simulation results from January 27 to 31, 2022. The  $T_{mfg}$  layer in both simulation and experiment demonstrates excellent consistency, with an Adjusted R-Square value of 0.983 and a maximum deviation of 2.61°C at noon. Regarding the temperature at the top position of the internal layer, the Adjusted R-Square value is 0.967, with the simulation result exhibiting a more significant fluctuation, including a maximum deviation of 4.04°C during the night and a maximum deviation of 4.09°C during daytime. In terms of the temperature difference between the outlet and inlet fluid temperature, which represents the energy harvesting capability, particularly from solar radiation, the Adjusted R-Square value is 0.915, with the maximum discrepancy between the simulation and experimental data reaching 5.14°C during daytime. The MAE, RMSE, STD and MBE is shown in Table 3.

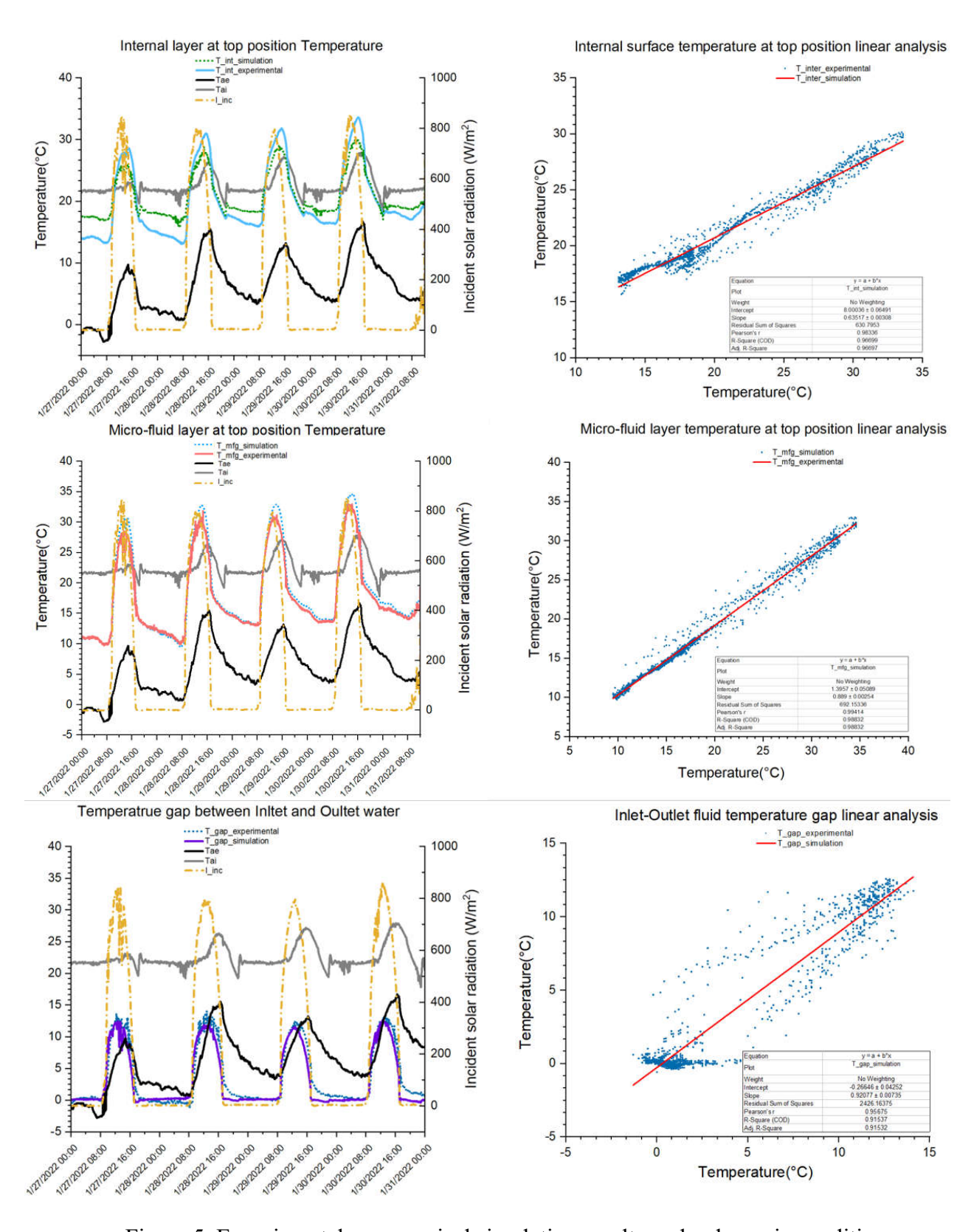


Figure 5. Experimental vs numerical simulation results under dynamic conditions

Table 3. Validation parameters

Index	MAE	RMSE	STD	MBE
$T_{inner}$	2.20	2.41	2.13	-1.14
$T_{difference}$	1.18	1.60	1.59	-0.22
$T_{mfg}$	1.04	1.47	1.43	0.32

# WHOLE BUILDING PERFORMANCE

The indoor space performance for the two simulation conditions is depicted in Figure 6. The results reveal that during summer, implementing the dynamic control strategy leads to a minor alteration in indoor air temperature, while a significant difference in surface temperature is observed. In winter, a noticeable temperature discrepancy is evident only during nighttime. The dynamic control strategy effectively reduces surface temperature while concurrently increasing the harvested solar radiation.

Table 4 presents the annual ideal energy need for heating and cooling as well as the annual solar radiation harvesting ratio. To facilitate a direct comparison of the energy performance of MFG, the performance of a Triple Glazing Unit (TGU) is also considered, albeit constructed within EnergyPlus rather than using co-simulation. This approach results in a slight variation in boundary conditions, but the TGU can still serve as a benchmark. The findings indicate that all conditions display relatively low ideal heating need due to efficient insulation, with values of 11.26 kWh/m<sup>2</sup> and 13.07 kWh/m<sup>2</sup>, which show minimal difference compared to the TGU value of 8.67 kWh/m<sup>2</sup>. Employing MFG offers significant advantages for ideal cooling need, as the circulating fluid can absorb a portion of the heat energy from solar radiation, thus mitigating overheating. Cooling needs are 36.3 kWh/m<sup>2</sup> and 34.45 kWh/m<sup>2</sup>, respectively, exhibiting a substantial reduction compared to the TGU value of 58.76 kWh/m<sup>2</sup>. Although the overall ideal heating and cooling need does not display a considerable difference between the dynamic and constant control strategies in this case, the flexibility of utilizing various control strategies underscores the potential for optimizing the dynamic control strategy. The annual solar radiation harvesting ratio consistently surpasses 20%, with the dynamic control strategy increasing the ratio from 23.08% to 24.26%. This highlights the substantial advantage of preventing overheating and implies potential opportunities for capitalizing on the heated fluid and optimizing the control strategy.

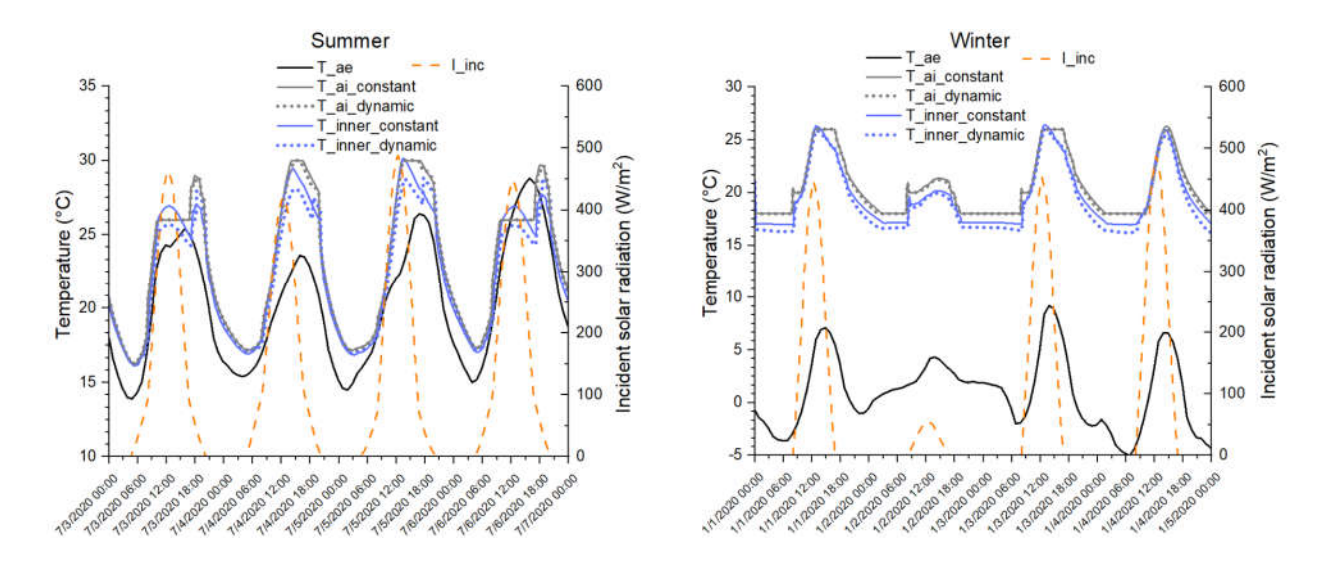


Figure 6. MFG performance under different control

Table 4. Annual performance under different condition

Control strategy	Energy need for heating	Energy need for cooling	Annual solar radiation harvesting ratio
	(kWh/m <sup>2</sup> )	(kWh/m <sup>2</sup> )	nar vosting ratio
Constant	11.26	36.3	23.08 %
Dynamic	13.07	34.45	24.26 %
TGU	8.67	58.76	0.00%

# **CONCLUSION**

In this study, a numerical model of triple glazing MFG technology has been developed and validated based on previous experimental research. The performance evaluation at the building scale was conducted through a co-simulation approach between the numerical model developed in Python Plugin and EnergyPlus. The numerical model demonstrates a relatively strong consistency with the experimental data for T<sub>inner</sub>, T<sub>mfg</sub> and T<sub>difference</sub>. However, during nighttime and noon hours, the internal surface temperature exhibits a maximum difference of 4.09°C, warranting further investigation to identify and reduce the discrepancy.

In terms of performance evaluation at the building level, the MFG technology demonstrates significant potential for energy savings and solar radiation harvesting, with approximately 47 kWh/m² for the entire year's ideal heating and cooling need. Implementing a dynamic control strategy enhances the annual solar radiation harvesting ratio to 24.26%. However, certain aspects still need deeper research, such as dynamic boundary conditions, long-wave radiation interactions with interior spaces, and potential applications for the heated fluid. Future research could delve into further optimization of MFG technology by integrating it with various control strategies and potentially incorporating it with HVAC systems.

# **ACKNOWLEDGMENT**

The research activities were carried out in the framework of POWERSKIN PLUS project. The project has received funding from the European Union's Horizon 2020 research and innovation program under Grant Agreement No. 869898.

# REFERENCE

- [1] E. C. Team, "Nearly zero-energy buildings." https://energy.ec.europa.eu/topics/energy-efficiency/energy-efficient-buildings/nearly-zero-energy-buildings en (accessed Apr. 23, 2023).
- [2] Directive 2010/31/EU of the European Parliament and of the Council of 19 May 2010 on the energy performance of buildings. 2010, p. 23. [Online]. Available: https://eur-lex.europa.eu/legal-content/EN/ALL/?uri=CELEX%3A32010L0031
- [3] M. Gutai and A. G. Kheybari, "Energy consumption of water-filled glass (WFG) hybrid building envelope," *Energy and Buildings*, vol. 218, p. 110050, Jul. 2020, doi: 10.1016/j.enbuild.2020.110050.
- [4] L. Xiangfeng and S. Tianxing, "Conceptual Development of Transparent Water Storage Envelopes," *Architectural Science Review*, vol. 50, no. 1, pp. 18–25, Mar. 2007, doi: 10.3763/asre.2007.5003.
- [5] L. Xiangfeng and S. Tianxing, "The Development of Transparent Water Storage Envelopes (TWSE) through Theoretical Thermal and Optical Analyses," *Architectural Science Review*, vol. 51, no. 2, pp. 109–123, Jun. 2008, doi: 10.3763/asre.2008.5115.
- [6] X. Liu, M. Xu, J. Guo, and R. Zhu, "Numerical study on the energy performance of building zones with transparent water storage envelopes," *Solar Energy*, vol. 180, pp. 690–706, Mar. 2019, doi: 10.1016/j.solener.2019.01.044.
- [7] B. P. V. Heiz, Z. Pan, G. Lautenschläger, C. Sirtl, M. Kraus, and L. Wondraczek, "Ultrathin Fluidic Laminates for Large-Area Façade Integration and Smart Windows," *Adv. Sci.*, vol. 4, no. 3, p. 1600362, Mar. 2017, doi: 10.1002/advs.201600362.
- [8] Manuela Baracani *et al.*, "Performance Assessment of a Microfluidic Glazing: Preliminary Results from a Winter Experimental Campaign," in 17th SDEWES Conference. 2022.
- [9] L. Su, M. Fraaß, M. Kloas, and L. Wondraczek, "Performance Analysis of Multi-Purpose Fluidic Windows Based on Structured Glass-Glass Laminates in a Triple Glazing," *Front. Mater.*, vol. 6, p. 102, May 2019, doi: 10.3389/fmats.2019.00102.
- [10] L. Su, M. Fraaß, and L. Wondraczek, "Design Guidelines for Thermal Comfort and Energy Consumption of Triple Glazed Fluidic Windows on Building Level," *Adv. Sustainable Syst.*, vol. 5, no. 2, p. 2000194, Feb. 2021, doi: 10.1002/adsu.202000194.
- [11] M. Fraaß and L. Su, "Modelling Fluidic Windows for Heating and Cooling," *J. Phys.: Conf. Ser.*, vol. 1425, no. 1, p. 012122, Dec. 2019, doi: 10.1088/1742-6596/1425/1/012122.
- [12] "ISO 15099:2003 Thermal performance of windows, doors and shading devices -- Detailed calculations." 2003. [Online]. Available: https://www.iso.org/standard/28790.html
- [13] W. M. Kays and M. E. Crawford, *Convective heat and mass transfer*, Third edition. in McGraw-Hill series in mechanical engineering. New York St. Louis San Francisco Auckland Bogotá Caracas

Lisbon London Madrid Mexico Milan Montreal New Delhi Paris San Juan Singapore Sydney Tokyo Toronto: McGraw-Hill, Inc, 1993.

- [14] Lawrence Berkeley National Laboratory, "WINDOW." 2022. [Online]. Available: https://windows.lbl.gov/tools/window/software-download
- [15] R. C. G. M. Loonen, F. Favoino, J. L. M. Hensen, and M. Overend, "Review of current status, requirements and opportunities for building performance simulation of adaptive facades," *Journal of Building Performance Simulation*, vol. 10, no. 2, pp. 205–223, Mar. 2017, doi: 10.1080/19401493.2016.1152303.
- [16] E. Taveres-Cachat, F. Favoino, R. Loonen, and F. Goia, "Ten questions concerning co-simulation for performance prediction of advanced building envelopes," *Building and Environment*, vol. 191, p. 107570, Mar. 2021, doi: 10.1016/j.buildenv.2020.107570.
- [17] G. Gennaro, E. Catto Lucchino, F. Goia, and F. Favoino, "Modelling double skin façades (DSFs) in whole-building energy simulation tools: Validation and inter-software comparison of naturally ventilated single-story DSFs," *Building and Environment*, vol. 231, p. 110002, Mar. 2023, doi: 10.1016/j.buildenv.2023.110002.
- [18] Robert H. Henninger and Michael J. Witte, "EnergyPlus Testing with ANSI/ASHRAE Standard 140-2001 (BESTEST)." Ernest Orlando Lawrence Berkeley National Laboratory, Jun. 2004.